JOURNAL OF APPLIED ELECTROCHEMISTRY 24 (1994) 808–813

Electrochemical characteristics of hydrogen storage alloys modified by electroless nickel coatings

K. NAITO, T. MATSUNAMI, K. OKUNO

Okuno Chemical Industries Co. Ltd., 1-10-25 Hanaten-Higashi, Tsurumi-ku, Osaka 538, Japan

M. MATSUOKA, C. IWAKURA*

Department of Applied Chemistry, College of Engineering, University of Osaka Prefecture, 1-1, Gakuen-cho, Sakai, Osaka 593, Japan

Received 15 October 1993; revised 3 December 1993

Multicomponent hydrogen storage alloy with the composition $MmNi_{3.31}Mn_{0.37}Al_{0.28}Co_{0.64}$ (Mm = misch metal consisting of 24.87% La, 52.56% Ce, 5.57% Pr, 16.86% Nd and 0.14% Sm) was used as a negative electrode material. To improve the performance of the negative electrode, the alloy particles were modified with various electroless Ni–P and Ni–B coatings. Electrochemical properties such as discharge capacity and high-rate dischargeability of the negative electrode were generally improved by the surface modifications. However, in the case of a Ni–P (10 wt % P) coating, the discharge capacity and high-rate dischargeability decreased with increasing thickness, due to the low hydrogen permeability and high electric resistivity of the coating. Consequently, both kinds of coating and their thickness are critical factors in determining the performance of such a negative electrode.

1. Introduction

Recently, extensive research into nickel–hydrogen batteries using hydrogen storage alloys as negative electrode material has been conducted because of their cleanness and high energy density [1–3]. Microencapsulation of the alloy particles with electroless copper or nickel coatings has been carried out to obtain further improvement of the performance of the negative electrode and this is very effective for preventing the deterioration of the disintegrated alloy particles and maintaining high electric conductivity [4–6]. In this work, a nonstoichiometric $AB_{4.6}$ compound, i.e., $MmNi_{3.31}Mn_{0.37}Al_{0.28}Co_{0.64}$ alloy was modified with various electroless Ni–P and Ni–B coatings and the coatings were characterized using electrochemical and physical methods.

2. Experimental details

$MmNi_{3.31}Mn_{0.37}Al_{0.28}Co_{0.64}$ alloy was prepared by arc melting and the alloy was divided into two particle sizes (20–25 μm and 106–125 μm) by passing through sieves after mechanical pulverization. The resulting alloy particles were modified with different electroless nickel coatings. The kind of electroless nickel coatings and conditions for surface modification are shown in Table 1. The quantity of the nickel coatings was varied between 5 and 20 wt % of the weight of the hydrogen storage alloy. Negative electrodes were prepared by the following procedure. After mixing the alloy particles (100 mg) with a small quantity of polyvinyl alcohol solution (2 wt % PVA), the mixture was loaded in a porous nickel substrate and then dried in vacuum before pressing it at 1200 kg cm^{-2}.

Electrochemical measurements were performed by the same procedure as reported previously [7]. Galvanostatic charge and discharge tests were made at 30° C using an unpressurized cell. The negative electrodes were charged for 2.5 h at 20 mA and discharged to −0.5 V vs Hg/HgO at the same current after leaving the electrode open circuit for 10 min. Such a cycle was repeated by the use of a galvanostatic charge–discharge unit (HJ-201, Hokuto Denko). The electrochemical capacity was calculated based on discharging time and expressed in mAh g^{-1} of hydrogen storage alloy.

The high-rate dischargeability was determined from the ratio of the discharge capacity measured at 200 mA (C_{200}) to the total capacity, being assumed to be the sum of C_{200} and C_{20} (the additional capacity measured at 20 mA). The high-rate dischargeability (%) is defined as $C_{200} \times 100/(C_{200} + C_{20})$.

A cross section of the negative electrode was examined by optical microscopy (Olympus, PMG3) to examine the effects of electroless nickel plating and cycling tests on the structure of the alloy particles.

The electric resistance of the electroless nickel coatings, which was plated on a nonconducting ceramic substrate (5 cm × 5 cm), was determined by the double bridge method using four point probes (Kyowa Riken, K-705RD). The internal stress of the electroless coatings was measured by use of a deposit

* Author to whom all correspondence should be addressed.

0021-891X

Table 1. Electroless nickel coatings used for surface modification of hydrogen storage alloy

Coatings	*Baths*	*Conditions*	*Coating quantity*
Ni–P (3.5 wt % P)	Top Nicoron SP–15*	85° C pH 4.7	20 wt %
Ni–P (10 wt % P)	Top Nicoron P–13*	85° C pH 6.0	5–20 wt %
Ni–B (0.4 wt % B)	Top Chem. Alloy B–1*	65° C pH 6.5	20 wt %
Ni–B (3.7 wt % B)	Niklad 740*	65° C pH 6.0	5–20 wt %

* Trade name of electroless plating solution produced by Okuno Chemical Industries Co. Ltd.

stress analyser (Electrochemical Company, 683EC) using a copper strip as the substrate. In addition, crystallographic characterization of the electroless nickel coatings plated on iron substrates was carried out using an X-ray diffractometer (Rigaku Denki, Rint-1100).

The diffusion coefficient of hydrogen in the electroless nickel coatings was determined by electrochemical measurements using electroless nickel foil as a bipolar electrode. The nickel foil, of thickness 10 μm, was prepared by peeling it off from the stainless steel substrate after the electroless plating. Detailed circuit and cell assembly for the measurements of diffusion coefficient were the same as reported by Devanathan and Stachurski [8]. In each run, hydrogen was galvanostatically charged from one side of the bipolar electrode and the penetrated hydrogen was potentiostatically oxidized on the other side. The buildup curve for the hydrogen oxidation was then measured as a function of time. After reaching the limiting current, the hydrogen charging circuit was opened, and the decay curve for the hydrogen oxidation was recorded. The diffusion coefficients, D, were calculated by using the following equation [9]:

$$D = 0.239L^2/t$$

where $t = (t_1 + t_2)/2$ and L is the thickness of nickel coating. t_1 is the time-lag in the buildup curve to reach 81% of the limiting current and t_2 is the time-lag in the decay curve to reach 19% of the limiting current.

3. Results and discussion

3.1. *Discharge capacity*

Figure 1 shows the discharge capacity of the negative electrodes with a particle size of 20–25 μm as a function of cycle number. The electroless nickel coatings were adjusted to 20 wt % of the weight of the hydrogen storage alloys. The saturation discharge capacity of the negative electrode consisting of unmodified alloy particles was substantially smaller than the calculated value based on the pressure composition isotherm [7]. However, the discharge capacity was increased by the modification of the alloy particles with electroless nickel coatings regardless of their kind. The maximum saturation discharge capacity was obtained by modification with a Ni–P (3.5 wt % P) coating since the microcurrent collection between the alloy particles and nickel substrate was remarkably improved.

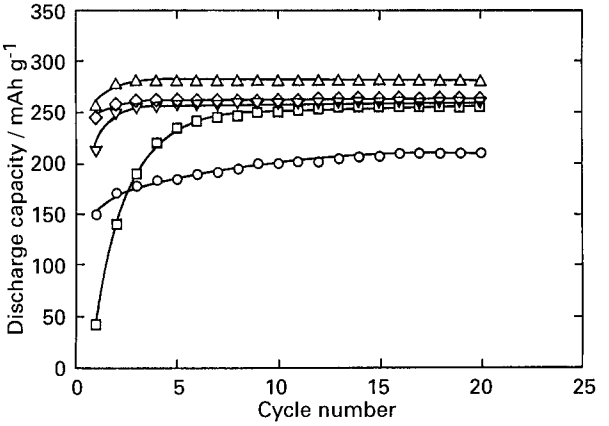

Fig. 1. Discharge capacity of the negative electrodes consisting of surface modified hydrogen storage alloy with a size of 20–25 μm. (○) Unmodified; (△) Ni–P (3.5 wt % P); (□) Ni–P (10 wt % P); (▽) Ni–B (0.4 wt % B); and (◇) Ni–B (3.7 wt % B).

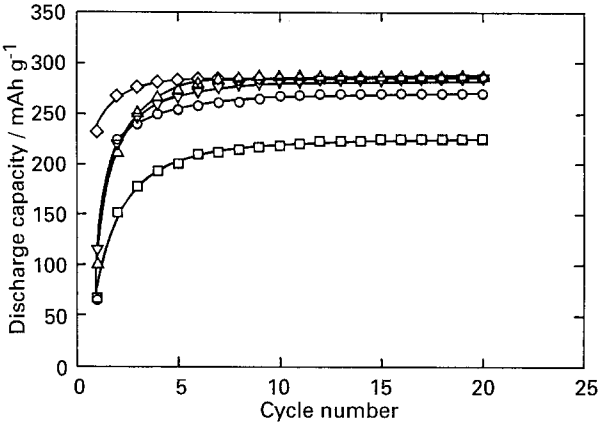

Fig. 2. Discharge capacity of the negative electrodes consisting of surface modified hydrogen storage alloy with a size of 106–125 μm. (○) Unmodified; (△) Ni–P (3.5 wt % P); (□) Ni–P (10 wt % P); (▽) Ni–B (0.4 wt % B); and (◇) Ni–B (3.7 wt % B).

Figure 2 shows the discharge capacity of negative electrodes consisting of alloy particles with a size of 106–125 μm as a function of cycle number. In this case, the amount of the electroless coatings was also kept at 20 wt %. The discharge capacity in the case of unmodified alloy particles was found to be 270 mA h g^{-1} at the 20th cycle. When the alloy particles were modified with Ni–P (3.5 wt % P), Ni–B (0.4 wt % B) and Ni–B (3.7 wt % B) coatings, the discharge capacity of the negative electrode increased to about 285 mA h g^{-1}. However, in the case of Ni–P (10 wt % P) coating, the discharge capacity was reduced and became smaller than that for unmodified alloy particles (225 mA h g^{-1}).

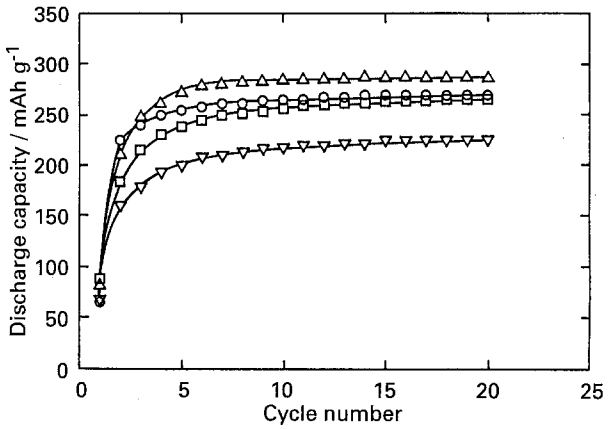

Fig. 3. Effect of surface modification with Ni–P (10 wt % P) coating on discharge capacity of the negative electrodes consisting of hydrogen storage alloy with a size of 106–125 μm. (○) Unmodified; (△) 5 wt %; (□) 10 wt %; and (▽) 20 wt %.

The thick Ni–P (10 wt % P) coating was different in the modification behaviour from the other electroless nickel coatings. Since the quantity of electroless coatings was kept constant, the coating thickness decreased with decreasing particle size. In order to elucidate the thickness effect of the Ni–P (10 wt % P) coating on discharge capacity, the quantity of electroless nickel coating was varied from 5 to 20 wt %. As shown in Fig. 3, the discharge capacity of the negative electrode, consisting of alloy particles with a size of 106–125 μm, was significantly increased by modification with Ni–P (10 wt % P) coating in small quantity (5 wt %) and then decreased with a further increase in coating thickness. This fact indicates that thick Ni–P (10 wt % P) coatings function as barrier films in charging and discharging. On the other hand, the thickness of the other electroless nickel coatings had little effect on the discharge capacity. Ni–P (10 wt % P) coatings were therefore quite different in terms of a strong dependence of the discharge capacity on the coating thickness.

3.2. *High-rate dischargeability*

The modification effect with various electroless nickel coatings on the high-rate dischargeability of the negative electrode is shown in Table 2. When the quantity of coatings was adjusted to 20 wt %, high-rate dischargeability of the negative electrodes was improved by surface modification of alloy particles with Ni–P (3.5 wt % P), Ni–B (0.4 wt % B) and Ni–B (3.7 wt % B) coatings. Although the modification with Ni–P (10 wt % P) coating reduced the high-rate dischargeability significantly, such a disadvantage could be eliminated by reducing the coating thickness. In the case of smaller particles (20–25 μm), improved high-rate dischargeability was obtained regardless of the kind of coatings. High-rate dischargeability in the case of smaller particles (20–25 μm) was generally larger than that obtained in the case of larger particles (106–125 μm), because of the shortened hydrogen diffusion path and increased effective surface area.

3.3. *Cross section of negative electrode*

The microscopic cross sections of negative electrodes, consisting of alloy particles with a size of 106–125 μm, before and after the cycling test, are shown in Fig. 4 and Fig. 5, respectively. Each alloy particle was uniformly covered with the electroless nickel coatings as can be seen in Fig. 4. In the case of Ni–B (3.7 wt % B) coating, significant disintegration was observed, but a crack-free cross section was observed in the modification with the other electroless nickel plating. After the cycling test, appreciable disintegration of alloy particles was detected regardless of the kind of coating, as shown in Fig. 5. However, in the case of the Ni–P (10 wt % P) coating, a few particles remained unchanged (Fig. 5(c)). This is one of the reasons for the reduction of the discharge capacity

Table 2. Effect of surface modification with electroless nickel coatings on high-rate dischargeability

Coatings	*Particle size*/μm	*Coating quantity*/wt %	*High-rate dischargeability*/%
Unmodified	20–25	0	77.3
Unmodified	106–125	0	76.5
Ni–P (3.5 wt % P)	20–25	20	83.2
Ni–P (3.5 wt % P)	106–125	20	79.9
Ni–P (10 wt % P)	20–25	20	82.9
Ni–P (10 wt % P)	106–125	5	79.4
Ni–P (10 wt % P)	106–125	10	75.7
Ni–P (10 wt % P)	106–125	20	66.3
Ni–B (0.4 wt % B)	20–25	20	88.9
Ni–B (0.4 wt % B)	106–125	20	78.4
Ni–B (3.7 wt % B)	20–25	20	90.2
Ni–B (3.7 wt % B)	106–125	5	81.2
Ni–B (3.7 wt % B)	106–125	10	81.7
Ni–B (3.7 wt % B)	106–125	20	80.0

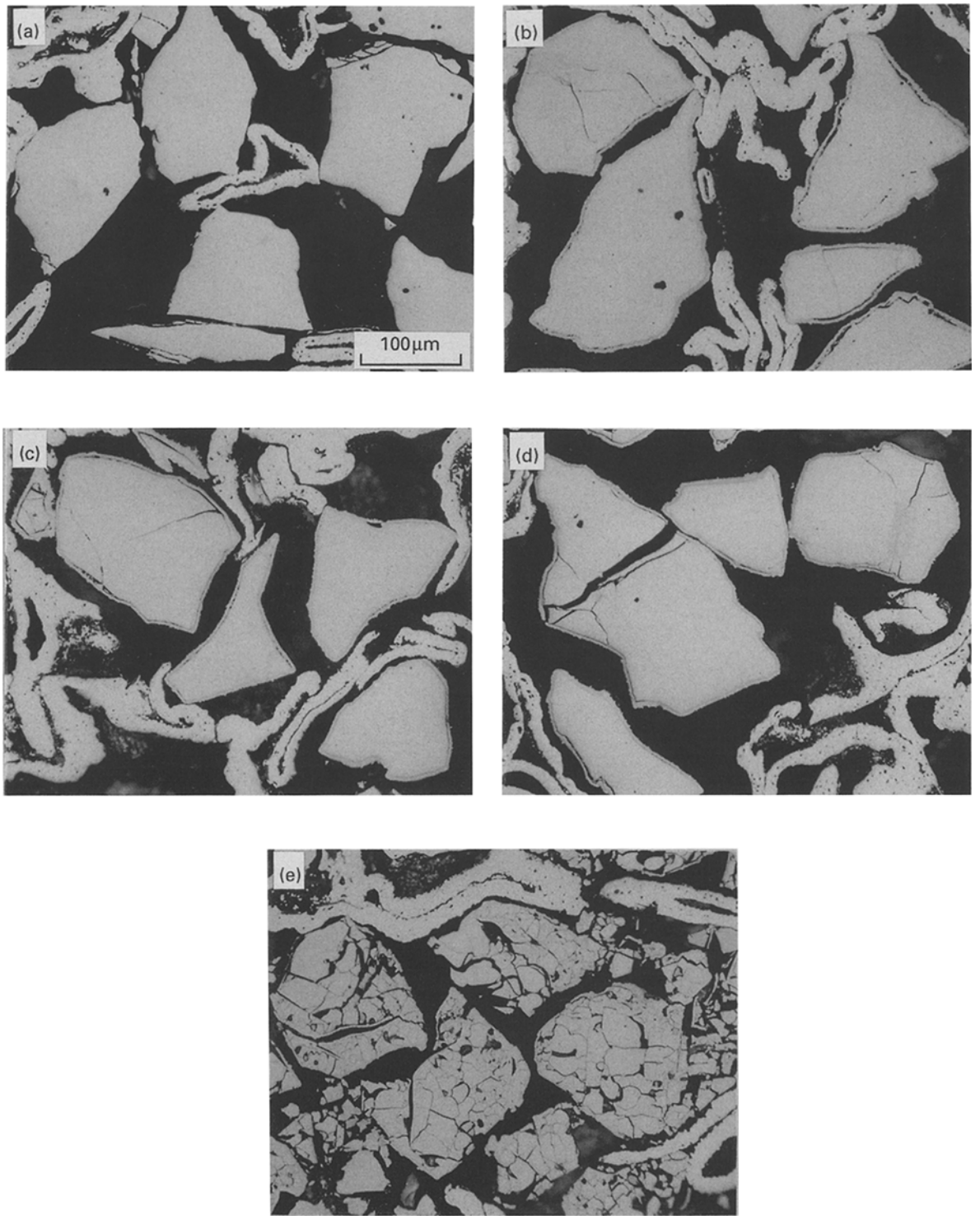

Fig. 4. Microphotographs of the cross section of negative electrodes before cycling. (a) Unmodified; (b) Ni–P (3.5 wt % P); (c) Ni–P (10 wt % P); (d) Ni–B (0.4 wt % B); and (e) Ni–B (3.7 wt % B).

in the modification with Ni–P (10 wt % P) coating. In contrast, disintegration of alloy particles is especially severe in the case of Ni–B (3.7 wt % B) coating, which increased the effective surface area. This is responsible for the rapid activation of the alloy particles [10]. The disintegration during electroless deposition of the Ni–B (3.7 wt % B) coating is probably induced by hydrogen penetration because of the extremely high concentration of reducing agent in the plating bath.

3.4. *Properties of electroless nickel coatings*

Typical X-ray diffraction patterns of the electroless nickel coatings plated on iron plate are shown in Fig. 6. In the case of the Ni–P (3.5 wt % P) coating, only one diffraction line corresponding to the Ni(1 1 1) plane was observed, whereas another diffraction line from the Ni(2 0 0) plane was also detected for Ni–B (0.4 wt % B) and Ni–B (3.7 wt % B) coatings. However, the Ni–P (10 wt % P) coating

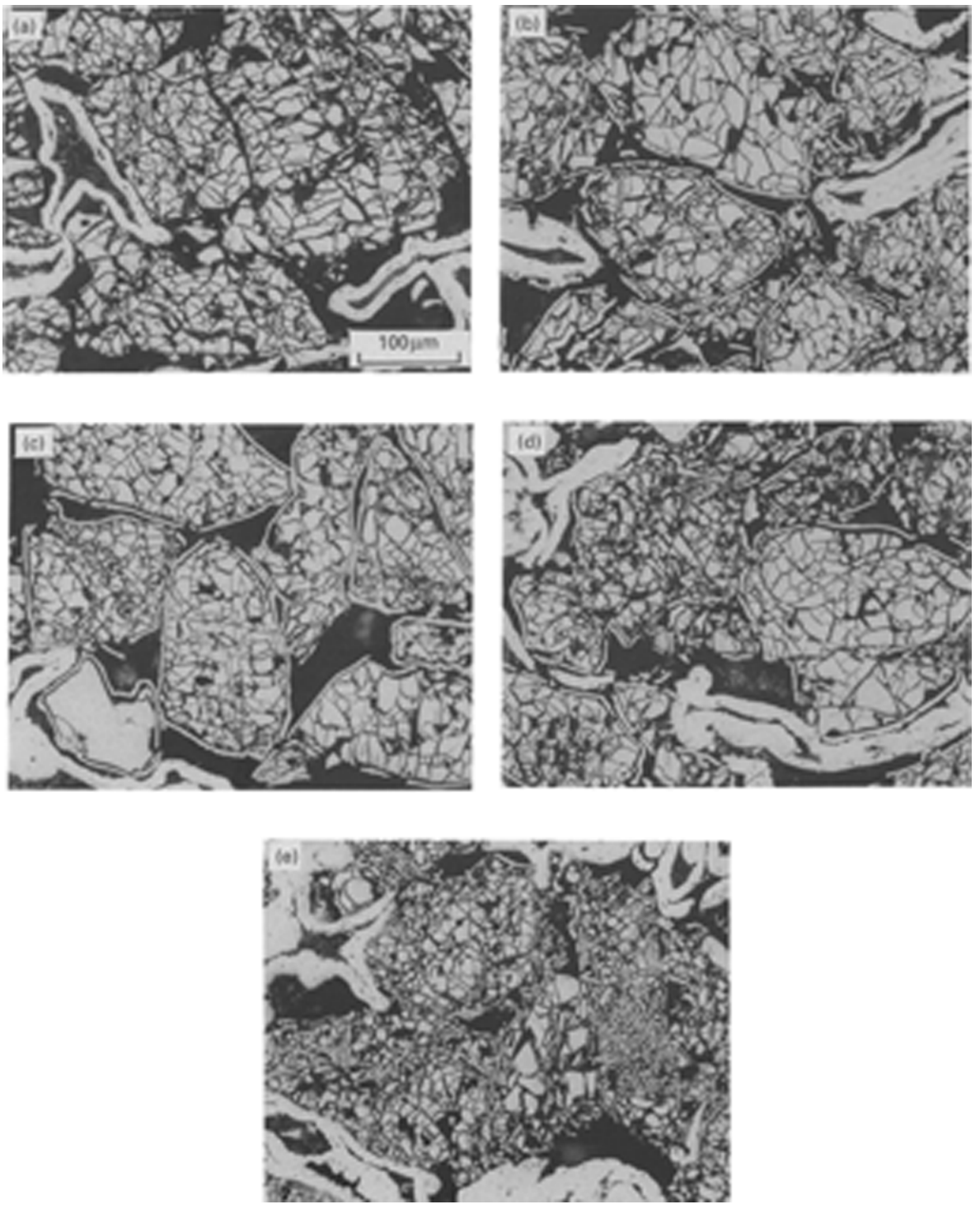

Fig. 5. Microphotographs of the cross section of negative electrodes after cycling. (a) Unmodified; (b) Ni–P (3.5 wt % P); (c) Ni–P (10 wt % P); (d) Ni–B (0.4 wt % B); and (e) Ni–B (3.7 wt % B).

Table 3. Properties of electroless nickel coatings used for surface modification

Coatings	*Resistance* /$\mu\Omega$ cm	*Internal stress* /kg mm^{-2}	*Diffusion coefficient* /cm^2 s^{-1}
Ni–P (3.5 wt % P)	67	6.5	6.4×10^{-10}
Ni–P (10 wt % P)	119	−5.2*	9.5×10^{-12}
Ni–B (0.4 wt % B)	27	28.4	4.8×10^{-10}
Ni–B (3.7 wt % B)	44	34.1	4.4×10^{-10}

* Negative value refers to compressive stress.

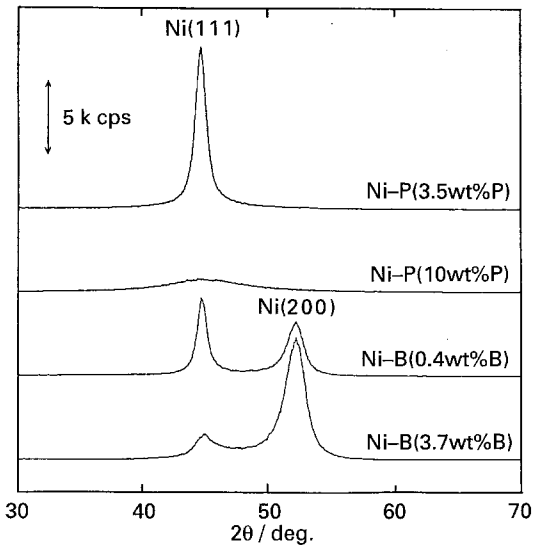

Fig. 6. X-ray diffraction patterns of electroless nickel coatings.

yielded a broadened diffraction line, giving evidence for an amorphous structure.

The diffusion coefficient of hydrogen, the electric resistance and the internal stress of electroless nickel coatings are summarized in Table 3. The Ni–P (10 wt % P) coating was characterized by high electric resistance and low hydrogen diffusion coefficient compared to the others. The diffusion coefficient of hydrogen in the Ni–P (10 wt % P) coating was found to be $9.5 \times 10^{-12}\,cm^2\,s^{-1}$, which was much smaller than that observed in the other electroless nickel coatings. Such a small diffusion coefficient was attributable to the amorphous structure of the Ni–P (10 wt % P) coatings, because the bulk diffusion of hydrogen was much slower than diffusion along grain boundaries [11]. In addition, the electric resistance of Ni–P (10 wt % P) coatings was considerably larger than those of the other coatings. In the case of the Ni–P (10 wt % P) coating, therefore, the thickness significantly affects the charge and discharge performance, since the small diffusion coefficient inhibits the penetration of hydrogen and the high electric resistance decreases the efficiency of microcurrent collection.

The internal stress of electroless Ni–P coatings was changed only slightly with phosphorous content, and was fairly small compared to the Ni–B coatings. As the Ni–B (3.7 wt % B) coatings had the maximum tensile stress, the disintegration of alloy particles was severe even before the cycling test, as mentioned previously. This indicates that the higher tensile stress will partly assist the hydrogen penetration into the alloy particle.

4. Conclusions

$MmNi_{3.31}Mn_{0.37}Al_{0.28}Co_{0.64}$ alloy of different particle size was modified with electroless Ni–P and Ni–B coatings. The modified alloy particles were used as negative electrode material. The effects of surface modifications on discharge capacity and high-rate dischargeability were examined. It was confirmed that the electrochemical properties of the negative electrode were significantly improved by the surface modifications, except for the thick Ni–P (10 wt % P) coating. An improvement in the electrochemical characteristics of the negative electrode was explained on the basis of the high efficiency of microcurrent collection and some disintegration of the alloy particles, giving rise to large effective surface area. In the case of thick Ni–P (10 wt % P) coatings, the electrochemical properties were severely impaired, because of the very small hydrogen diffusion coefficient and the high electric resistivity. In this case, coating thickness is a critical factor in determining the performance of the negative electrode. However, this disadvantage was eliminated by reducing the quantity of electroless Ni–P (10 wt % P) coating to 5 wt % of the weight of hydrogen storage alloy.

Acknowledgement

This work was partly supported by a grant-in-aid for Developmental Scientific Research (No. 05555172) from the Ministry of Education, Science and Culture of Japan.

References

[1] J. J. G. Willems, *Philips J. Res.* **39** (1984) 1.
[2] C. Iwakura and M. Matsuoka, *Kidorui (Rare Earth)*, No. 17 (1990) pp. 11–36.
[3] *Idem, Prog. Batteries and Battery Mater.* **10** (1992) 81.
[4] C. Iwakura, T. Asaoka, T. Sakai, H. Ishikawa and K. Oguro, *Denki Kagaku* **53** (1985) 722.
[5] T. Sakai, H. Ishikawa, K. Oguro, C. Iwakura and H. Yoneyama, *J. Electrochem. Soc.* **134** (1987) 558.
[6] C. Iwakura, M. Matsuoka, K. Asai and T. Kohno, *J. Power Sources* **38** (1992) 355.
[7] K. Naito, T. Matsunami, K. Okuno, M. Matsuoka and C. Iwakura, *J. Appl. Electrochem.* **23** (1993) 1051.
[8] M. A. V. Devanathan and Z. Stachurski, *Proc. Roy. Soc.* **A270** (1962) 90.
[9] J. McBreen, L. Nanis and W. Beak, *J. Electrochem. Soc.* **113** (1966) 1218.
[10] M. Matsuoka, H. Mori, K. Asai and C. Iwakura, *Chem. Express* **7** (1992) 189.
[11] M. Matsuoka, S. Maegawa and C. Iwakura, *Hyomen Gijutsu* **41** (1990) 706.